NASA/TM–2018-220082

Probabilistic Sensitivity Analyses Incorporating Surrogate Models for the Structural Response of a Representative Inflatable Space Structure

Karen H. Lyle and Thomas C. Jones
Langley Research Center, Hampton,Virginia

August 2018

NASA STI Program . . . in Profile

Since its founding, NASA has been dedicated to the advancement of aeronautics and space science. The NASA scientific and technical information (STI) program plays a key part in helping NASA maintain this important role.

The NASA STI program operates under the auspices of the Agency Chief Information Officer. It collects, organizes, provides for archiving, and disseminates NASA's STI. The NASA STI program provides access to the NTRS Registered and its public interface, the NASA Technical Reports Server, thus providing one of the largest collections of aeronautical and space science STI in the world. Results are published in both non-NASA channels and by NASA in the NASA STI Report Series, which includes the following report types:

- TECHNICAL PUBLICATION. Reports of completed research or a major significant phase of research that present the results of NASA Programs and include extensive data or theoretical analysis. Includes compilations of significant scientific and technical data and information deemed to be of continuing reference value. NASA counter-part of peer-reviewed formal professional papers but has less stringent limitations on manuscript length and extent of graphic presentations.

- TECHNICAL MEMORANDUM. Scientific and technical findings that are preliminary or of specialized interest, e.g., quick release reports, working papers, and bibliographies that contain minimal annotation. Does not contain extensive analysis.

- CONTRACTOR REPORT. Scientific and technical findings by NASA-sponsored contractors and grantees.

- CONFERENCE PUBLICATION. Collected papers from scientific and technical conferences, symposia, seminars, or other meetings sponsored or co-sponsored by NASA.

- SPECIAL PUBLICATION. Scientific, technical, or historical information from NASA programs, projects, and missions, often concerned with subjects having substantial public interest.

- TECHNICAL TRANSLATION. English-language translations of foreign scientific and technical material pertinent to NASA's mission.

Specialized services also include organizing and publishing research results, distributing specialized research announcements and feeds, providing information desk and personal search support, and enabling data exchange services.

For more information about the NASA STI program, see the following:

- Access the NASA STI program home page at http://www.sti.nasa.gov

- E-mail your question to help@sti.nasa.gov

- Phone the NASA STI Information Desk at 757-864-9658

- Write to:
  NASA STI Information Desk
  Mail Stop 148
  NASA Langley Research Center
  Hampton, VA 23681-2199

NASA/TM–2018-220082

Probabilistic Sensitivity Analyses Incorporating Surrogate Models for the Structural Response of a Representative Inflatable Space Structure

Karen H. Lyle and Thomas C. Jones
Langley Research Center, Hampton,Virginia

National Aeronautics and
Space Administration

Langley Research Center
Hampton, Virginia 23681-2199

August 2018

Available from:

NASA STI Program / Mail Stop 148
NASA Langley Research Center
Hampton, VA 23681-2199
Fax: 757-864-6500

Abstract

This study concentrates on results from probabilistic analysis and numerical simulation tools to identify parameter sensitivities and assess surrogate model suitability for a novel inflatable airlock concept, specifically the Non-Axisymmetric Inflatable Pressure Structure (NAIPS) under NASA's Minimalistic Advanced Softgoods Hatch (MASH) Program. The current studies extended the demonstration of probabilistic analysis tools to identify parameter sensitivities by: incorporating nonlinear material load-strain property curves and orthotropic representation of the fabric; and exploring the use of surrogate models to facilitate rapid evaluations as new information becomes available, as well as enable optimizations. The airlock model has been simplified to focus on the end dome section. Brief overviews of the finite element model and associated surrogate models are provided along with the probabilistic sensitivity analysis approaches. Responses of interest include the sensitivities of various loads in the structural elements of the NAIPS to material properties, cord lengths, inflation pressure and friction between softgoods components. The use of surrogate models was explored to facilitate rapid sensitivity evaluations as parameter ranges change. The completion of the sensitivity studies improved understanding of the dependence of load responses to several uncertain parameters and confidence in the ability to use surrogate models to represent the finite element simulations.

Introduction

High-reliability, inflatable space structures are in demand for a number of applications due to their efficient packaging and light weight. Traditionally, evaluations and validation of design concepts have been performed through testing because of the limited analysis capability for softgoods structures. However, recent advances in simulation capability and computational speed have enabled simulations of a wide range of aerospace applications. Examples where numerical simulations were utilized in soft-goods applications include: inflatable habitats such as the Bigelow Expandable Activity Module (BEAM)[1,2]; atmospheric decelerators such as the Hypersonic Inflatable Aerodynamic Decelerator (HIAD)[3,4]; attenuation systems such as the Orion Crew Module Airbag Landing System[5,6]; and aerospace recovery systems[7].

Sensitivity analyses are performed for a number of reasons. For example, analyses are used to identify, in a quantitative manner, the variables that control the variation in responses. With this knowledge, designers can direct resources to reduce uncertainties in point-designs, as well as to utilize the results to efficiently modify designs to improve performance. Sensitivity analyses can also be used for screening variables, i.e., to down-select from a large list of parameters to the most significant variables that will be incorporated into future analyses. At the outset of these studies, it was desired to identify those parameters that could control variations in the load responses by generating sensitivity results incorporating uncertainty models. This information could then be used to improve comparisons of simulation results with test data. A

review of many sensitivity methods and applications can be found in Ref. 8.

Complementary to the advances in structural computational capabilities has been the implementation of probabilistic methods and establishment of standards for verification and validation of numerical simulations. Several technical societies and agencies are developing standards for documenting the uncertainty of responses to variations in input parameters[9-11]. Probabilistic Analysis (PA) methods can be used to support sensitivity studies in a number of phases of design. For example, parameter variations and their representation can be selected based on expected parameter deviations from the as-built system. In addition, PA tools can be used to conduct parametric studies where the uncertainty model description represents a design space, as opposed to an uncertainty space. For probabilistic analyses, sophisticated methods may be required to optimally use the results from a relatively small number of simulations. The choice of method is dependent on the number of uncertain parameters, the number and types of responses, the simulation execution time, and the physics of the application. Examples of aerospace applications incorporating probabilistic methods are provided in Refs. 12 and 13.

As NASA continues to explore the use of inflatables for a variety of applications, development of a certification plan for the human-rated inflatable space structure is critical[14]. Robust analysis techniques for inflatables need to be explored and verified so they can be incorporated into the design and certification of future softgoods structures. A novel inflatable airlock concept, specifically the Non-Axisymmetric Inflatable Pressure Structure (NAIPS) under the Minimalistic Advanced Softgoods Hatch (MASH) Program[15,16], is the application focus of this report, see Figure 1. The NAIPS structural analysis problem represents many design challenges, including: 1) the lack of formal design approaches to address such softgoods hatch concepts; and 2) modeling the behavior of complex structural responses that include uncertainty in soft goods material properties and transfer of loads through multiple paths and different softgoods elements. Fortunately, the detailed computational tools needed to analyze the structural response of such systems are becoming sufficiently mature to adequately model the response of these complex structures. Additionally, it is now feasible to complete the numerous nonlinear transient dynamic simulations that are critical to support verification of the design in a reasonable amount of time.

A preliminary series of studies focusing on end-state loads in the NAIPS inflatable habitat, was reported in Ref. [17]. The current studies extend the demonstration of probabilistic analysis tools to identify parameter sensitivities by: incorporating nonlinear material load-strain property curves and orthotropic representation of the fabric; and exploring the use of surrogate models to facilitate rapid evaluations as new information becomes available as well as enable optimizations. Responses of interest include the cord loads and fabric line-loads. A brief overview of the finite element model (FEM) and the probabilistic analysis approaches is provided, which is followed by a discussion of the results. Within the discussion of the results, parameter sensitivities are computed from FEM simulations as well as from surrogate models. Finally,

concluding remarks provide general comments about the approaches and findings.

Description of Inflatable Hatch Concept

NAIPS is an inflatable airlock and soft hatch concept that consists of high-specific strength Vectran fabric constrained by a network of braided Vectran cords, see Figure 1. The concept dimensions were selected to provide adequate room for two astronauts to don and doff their space suits as they transfer between the pressurized spacecraft and the vacuum of space. The design utilizes the ability to transfer the internal pressure load applied to the woven fabric to the cords, which are then capable of carrying the majority of the load. Additionally, the design takes advantage of the low-stress areas in the lobes of each end dome perpendicular to the dome radial (or meridional) cords. These low stress regions enable inclusion of one or more lightweight soft hatch openings, analogous to a zipper. Mechanical property tests were performed on the fabric and the cords to obtain load-strain properties. It should be noted that the woven fabric and braided cords undergo large displacements at the onset of loading, due to decrimping and untwisting of the yarns, in addition to material strain. The load-strain behavior also changes as the materials are cyclically loaded through the pressurization / depressurization of the airlock. Prior to this analysis effort, experiments were conducted to acquire structural response data for a representative, full-scale point design. Additional details about the EDU design, test data and early simulation results were provided in Ref. 16.

Description of Analyses

Finite Element Model (FEM)

The sensitivity studies required a model that was numerically stable and efficient enough that hundreds of simulations could be completed in a short period of time. For this project, a short period of time was expected to be 1 to 2 weeks, with an execution time for a single simulation of a few hours. An existing full model was simplified by extracting a quarter symmetry section of the dome. The simplified FEM contained 10,144 nodes, with 8,960 fully-integrated shell elements and 1160 2-noded beam elements. The numerical simulations were executed in LS-Dyna[18], a commercial, general-purpose, nonlinear, transient-dynamic, finite element code. The previous report[17] that focused on a linear elastic quarter symmetry model, contains suggestions and lessons learned that mitigated much of the numerical instabilities. As a result, the models executed for these studies were numerically stable for all of the parameter combinations (total of 380 FEM simulations).

A brief summary of the model is provided here. The FEM representation of the NAIPS dome section, with symmetry boundary conditions identified, is shown in Figure 2a. The model is composed of an orthotropic fabric constrained by a network of radial cords attached to a loop (or axial) cord. All of the materials are represented by nonlinear load-strain curves derived from test data. Two radial cord configurations were simulated as shown in Figure 2b. The top figure

shows an inflated end-state of the model with 11 radial cords (replicating the as-tested NAIPS configuration) while the bottom figure shows a 6-cord configuration that was also studied here for comparison. For the 6-cord configuration, the 11-cord model was modified by simply removing the intermediate radial cords. Additional details about the modeling approach and lessons learned are also provided in Ref. 17.

At the start of the simulations, the article is deflated and flattened (Figure 2a), and the radial cords are sized to where their midpoint lies at the radius of the dome, with an initial cord length of 111 in. These cords were then shortened during inflation, through the inclusion of thermal loading applied to elements at each end of the radial cords, where they attach to the loop cord. A negative temperature change is applied to the 2-noded beam elements, referred to here as "thermal elements" to contract them, see Figure 2a. To retain uniform axisymmetric behavior, all of the radial cords are shortened to the same length. This shortening is performed to simulate the as-fabricated cord lengths, which are shorter than the initial model state. The shortened cords induce the formation of the lobes and transfer much of the load from the fabric to the radial cords. Contact definitions are crucial to the simulations by enabling transfer of loads between the parts. All of the contacts are penalty-based, where the friction and penalty-force stiffness scale factors can be varied. The material models were selected to replicate the behavior of the woven fabric and braided cord materials.

The normalized profiles for both the pressure and the thermal loads used in all simulations are shown in Figure 3. The pressure load (or inflation pressure) is applied to the fabric inner surface and linearly increased from zero to a prescribed value over the time range from 0 to 0.3 seconds. The primary goal of the history profile for the pressure load was to enable "inflation" while also minimizing execution time and minimizing unwanted transient dynamic behavior. The profile is not intended to replicate the actual inflation time of the airlock. It should be noted that the material damping was increased during the initial pressure loading to minimize transient dynamic behavior. Concurrently, a linear temperature decrease is applied to the thermal elements from 0 to 0.15 seconds. The thermal elements are a numerical feature that enables inclusion of cords of varying lengths in a numerically stable manner. The simulations are executed until 0.4 s to allow the loads to reach equilibrium and mitigate dynamic effects.

The clock time to compute the 0.4-second responses was approximately 2 hours using 8 processors. Unlike most applications using an explicit, transient-dynamic analysis, only the end-state results, and not the time-varying responses, were of interest. Figure 4 contains a schematic of the inflated model with the responses identified. The following results for each simulation were saved: loads for each of the radial cords (P_{RC}); loads at 3 locations along the loop cord (P_{LC}); and the radial and tangential line-loads (N_R and N_T, respectively) for each of the lobes, computed from the elemental stresses of representative elements near the equator.

Sensitivity Analyses

The sensitivity analyses results are dependent on a selection of the sampling approach, parameter bounds, sensitivity metric and whether to directly use FEM simulations or surrogate models derived from simulations. Although there are many techniques that can create adequate sampling of the parameter space for a probabilistic analysis, Halton-Leap deterministic sampling[19] was chosen for this study. The Halton-Leap method creates uncorrelated, multi-dimensional, uniformly distributed values between 0 and 1, which are then converted to engineering values. A total of 6 parameters were varied in each of the probabilistic sets via 3 sub categories: 1) Material properties through multiplicative factors on the ordinate of each of the load-strain curves: radial cord (F_{RC}), the dome fabric (F_F), and the loop cord (F_{LC}). 2) Geometric parameters through changes in the radial cord length (L_{RC}). 3) Operating parameters through changes in the inflation pressure (P), and the contact friction (μ) between the dome fabric and the radial cords. The bounds on the material load-strain curves, and the friction and pressure remained the same for all of the analyses. Figure 5 graphically illustrates the impact of the factors on the load-strain curves. The uncertainty factor was applied to the load (or ordinate) values. The parameter ranges were based on engineering judgments, with an expectation that the bounds could be adjusted as additional information became available.

There are a number of methods for computing sensitivities and ranking variables. These include local gradient-based methods[20], and global techniques[21,22]. From previous experiences with inflated fabric structures, the global correlation method has proven to be acceptable for understanding the importance of variables, even under large deformations and nonlinear stress-strain behaviors[13]. As with all studies, the project's required accuracy or adequacy needs are critical to determining which approach is best suited to the application. If a correlation approach is not sufficient, then more sophisticated approaches incorporating surrogate models and global sensitivity methods, such as Sobol[22], may be needed. The Sobol method is a variance-based computation that is often used to compute global sensitivities for non-linear as well as linear systems. The global sensitivities are usually represented as a percentage of the total response variance.

Applications that require a quick turn-around can greatly benefit from the generation of a surrogate model. For example, a probabilistic analysis set of FEM simulations can require days or weeks to complete. Subsequently, when sensitivity results for a refined set of parameters is desired or optimizations are needed, a surrogate model could be generated and quickly interrogated. In addition, variance-based global sensitivity measures such as Sobol often need a large number of response samples (i.e., thousands) to compute the variance. For the current application, it is possible to compute 10,000 responses in minutes using the surrogate model, where 10,000 FEM simulations would take orders of magnitude longer. These global sensitivities take into account not only the gradient but also the range or standard deviation of the input parameters. Two surrogate model methods have been explored for this application: the

Extended Radial Basis Function (ERBF) approach developed by Mullur and Messac[23]; and a second-order response surface method[24] (RSM). A sample point includes a unique set of parameter input values and the response is a set of outputs of interest which include cord loads and fabric line loads. A surrogate model describes the relationship between the sample input sets and one of the outputs of interest. Thus, for the 11-cord configuration, 34 surrogate models (11 P_{RC}, 3 P_{LC}, 10 N_R, 10 N_T) were needed, while for the 6-cord configuration 19 surrogate models (6 P_{RC}, 3 P_{LC}, 5 N_R, 5 N_T) were needed. Sensitivity analyses were computed using both user-written Matlab[25] scripts as well as LS-Opt[26], a commercially availability software package.

Discussion of Results

Table I provides input parameter information for the 4 analysis sets, designated as Sets D, E, F, and G that will be examined (Results for Sets A-C are contained in Ref. 17). The only parameters that change, highlighted in bold in the table, are the number of radial cords (11 vs 6) and the range for the radial cord length (L_{RC}). The NAIPS EDU consisted of radial cords spaced at 18-degree increments, which results in 11 cords for the dome symmetry-model. The smaller range for L_{RC} (Set E) corresponds more closely to the as-tested configuration.

A common format has been used for presentation of the sensitivity results herein. Each figure is subdivided into a 2 x 2 grid of plots. Specifically, the upper left (subplot a) corresponds to the radial cord loads (P_{RC}); the upper right (subplot b) to loop cord loads (P_{LC}); the lower left (subplot c) to lobe radial line-loads (N_R); and the lower right (subplot d) to lobe tangential line-loads (N_T).

Results for NAIPS radial cord configuration (11 cords)

Figure 6. shows the Set D sensitivity results in the form of the magnitude of the correlation coefficients, $|R|$. The $|R|$ values were computed directly from the results of 140 simulations. The standard error for $|R|$ is based on the number of samples, which for 140 samples is approximately 0.1. These results show that the radial cord length, L_{RC} (yellow), is the single dominant parameter for all responses. As noted earlier, the relatively large variation in L_{RC} was intended to generate a set of simulations that could span a larger design space. However, in construction of a habitat, it is highly unlikely that the fabricated radial cord length would vary as much as specified. Since L_{RC} dominated this sensitivity analysis, it was desired to understand if other parameters would become important if control on L_{RC} was tightened. Since parameter set E is encompassed by that in Set D, Extended Radial Basis Function (ERBF) surrogate models were generated to study their effectiveness at approximating the results of what would otherwise be an additional large set of FEM analysis runs.

When working with surrogate models, users should always be concerned about their accuracy. Since results from 140 FEM simulations (requiring 10 days to complete) were already available, these results were used to assess the accuracy of the surrogate models. This

assessment was performed by removing the *ith* LS-Dyna solution from the solution set and comparing it to the surrogate prediction, as depicted in Figure 7. In other words, the surrogate model did not contain the *ith* solution being evaluated. The removal process was performed with all 140 LS-Dyna FEM solutions for each of the 34 load and line load responses of Set D. Results of the comparison between the simulation and surrogate model responses are shown in Figure 8. In each graph the ERBF load response is plotted on the abscissa, while the FEM simulation results are plotted on the ordinate axis. For example, the comparisons for P_{RC} are provided in the upper left graph (subplot a) for each of the 11 radial cord loads and all 140 simulations (i.e., the figure contains a total of 1540 symbols). Using visual inspection, the comparison between the ERBF approximations and the simulation results in each of graphs (a-d) looking qualitatively "very close". However, a quantitative comparison was desired. Thus, the error of the ERBF was calculated for each of the 34 loads, by computing the RMS error and then normalizing the error by the mean, see Table II. These errors, all less than 2%, were considered small enough to use the ERBF for further computations. However, if this level of agreement were deemed insufficient, new simulation results can be incorporated to improve the surrogate's accuracy or a different surrogate model method (such as Kriging) could be used. In addition, this level of accuracy suggests a smaller number of simulation cases could be used in the surrogate models if the required error was set higher, say at 5%.

Taking the surrogate models generated from Set D and applying the ranges specified for Set E, the $|R|$ values were computed, see Figure 9. In contrast to Set D results, the results for Set E show a significant influence on the loads from 3 parameters, namely the F_{RC}, L_{RC}, and F_F. In addition, a fourth parameter, P, also exhibits a significant correlation for several loads.

As this was the first use of a surrogate model for this type of application, an additional 100 simulations were executed based on the parameter ranges for Set E. In Figure 10, the $|R|$ values for the FEM simulations have been cross-plotted against the $|R|$ values based on ERBF approximations. Based on the number of samples, it is anticipated that variations of less than 0.1 are not significant. The use of surrogate models is appropriate for further use based on: the small normalized RMS errors provided in Table II; and confirmed by the closeness of the $|R|$ values of the ERBF relative to the simulations. The surrogate models not only predict the loads adequately, but also correctly identify and highlight the relative importance of the input parameters on those responses.

As stated previously, there are several options for assessing sensitivities other than correlation coefficients, $|R|$, as well as several options for producing surrogate models. In fact, examining multiple approaches for computing sensitivities is preferred, particularly when applied to new applications. To facilitate comparisons of different methods, one representative response of each type was extracted - namely, radial cord load #5 (P_{RC}^5), loop cord load #2 (P_{LC}^2), line-loads for lobe #5 (N_T^5 and N_R^5), see Figure 2b. The dominance of one parameter (L_{RC}) in Set D would minimize the ability to distinguish subtleties of each method. Therefore, the focus for the

sensitivity comparisons was Set E. Figure 11a contains the $|R|$ values computed from 100 simulations for Set E, extracted from data in Figure 10. As results for $|R|$ for the ERBF surrogate models have been compared in Figure 10, an alternative, and widely used, surrogate model method was exercised, specifically, a 2nd-order response surface method (RSM). Response Surface Method surrogate models were generated from Set D FEM simulations. The RMS errors for these surrogate models are provided in the table in the lower right of Figure 11. These RSM surrogate models were then evaluated at the Set E parameters. A correlation coefficient was computed from the 100 RSM approximations for each representative response, shown in Figure 11b. The top three sensitivity parameters for the responses are the same. However, a difference in order of sensitivity for F_F and L_{RC} has been noted. Another way to compute sensitivities is through Sobol contribution to the variance. For direct comparison with subplot (a), RSM surrogate models were generated using Set E simulations. The RMS errors for the Set E surrogate models are also provided in the lower right table. Instead of assessing sensitivity based on correlation coefficients, the sensitivities are based on the Sobol method, see Figure 11c. The Sobol results are typically normalized such that the total contribution is 100%, thus direct comparison of magnitudes of $|R|$ with Sobol results is not appropriate. The results for the top three contributors to the response variation are in the same order as for Figure 11a.

Effect of reducing number of radial cords

Finally, the impact of changing the number of radial cords was examined. This is one of the considerations a designer of this type of inflatable architecture may need to analyze. The existing model was readily modified by removing alternate radial cords, such that 6 radial cords remained. The |R| values for Set F, see Figure 12, are similar to those for Set D in that L_{RC} dominates the sensitivities. Based on the confidence gained in the previous section for the 11-cord configuration, ERBF surrogate models were generated for the Set F simulations. In a similar manner, the comparisons of ERBF surrogate model results with Set F simulations are cross-plotted in Figure 13. The corresponding summary of the normalized RMS error is provided in Table III. It is noted that comparisons of N_T for Lobe 5 (Figure 13d – green squares), showed significantly higher discrepancy than the other 18 responses. To better understand this behavior, N_T for Lobe 5 has been cross-plotted against each of the 6 input parameters (Figure 14) for both the FEM simulations and ERBF approximations. N_T approaches zero asymptotically as L_{RC} increases (subplot c). This means that at the mid-lobe location near the equator, the tangential line-lobe is very small. It should also be noted that “wrinkling” of the fabric was occurring near the equator. Wrinkling of the fabric in the lobes was not observed for the 11-cord configuration. To assess the relationship between L_{RC} and N_T for all lobes, the cross-plots are shown in Figure 15. As seen in Table III, the error of N_T for lobes 1 and 4 was substantially higher (5%) than the other responses. The magnitude of the error is directly related to the magnitude of N_T for L_{RC} > 107 in. The correlation coefficients computed using the Set F ERBF surrogate models with the Set

G parameters are shown in Figure 16. A low |R| value for Lobe 5 N_T (Figure 11d) is noted. This could be anticipated from review of Figure 14d, where Lobe 5 N_T is insensitive to L_{RC} for L_{RC} > 107 in.

The primary reason for evaluating sensitivities for the 6-cord configuration was to understand the impact of cord number on the parameter sensitivities. In other words, does the number of cords impact the conclusions about where to place resources to minimize response uncertainty. It is understood that changing the number of cords will impact the magnitude of the cord loads and the cord-to-fabric load sharing. Comparisons of the sensitivities of the 11-cord and 6-cord configurations are provided in Figure 17. Results for a middle lobe, away from the boundaries were selected. For the 11-cord configuration, these are the radial cord 5 (P_{RC}^5), loop cord 2 (P_{LC}^2), and Lobe 5 results (N_T^5 and N_R^5). For the 6-cord configuration, these are: the radial cord 3 (P_{RC}^3), loop cord 2 (P_{LC}^2), and Lobe 3 results (N_T^3 and N_R^3). In general, the sensitivities are similar for the two configurations. However, a difference is noted for the lobe radial line-load (N_R) identified in Figure 17. For this response, the sensitivity to pressure is larger for the 11-cord configuration when compared to the concept with 6-cords. In contrast L_{RC} is less important for the 11-cord configuration when compared to the 6-cord results.

Concluding Remarks

The studies summarized in this report follow an initial series of studies that demonstrated the use of uncertainty-based numerical simulation for a linear, isotropic symmetry model of an inflatable airlock design. This study concentrates on the utilization of probabilistic analysis tools that include surrogate models for FEMs that contain nonlinear load-strain curves and orthotropic fabric representation. The simulation of the response of the airlock structure to pressure loading was automated using Matlab scripts to control the LS-Dyna simulations. The global sensitivity of the component loads was computed using multiple metrics computed using user-written scripts and commercial software.

A model was simplified to reduce computation time while retaining important behaviors. Specifically, an axisymmetric model of the NAIPS dome was derived from a full model. This model kept features, such as using thermal loads to shorten cords and the special contact available in LS-Dyna for guiding cables on surfaces. Responses of interest were the cord loads and fabric line-loads.

In summary:

- Implementation of the lessons learned regarding numerical stability from the earlier studies enabled the successful completion of all 380 FEM simulations.
- Initial parameter ranges produced results where the radial cord length dominated the sensitivity results for all loads examined.
- Surrogate models were generated from the initial simulations. The surrogate models were assessed for adequacy and subsequently used to understand sensitivities once the radial cord

length parameter range (L_{RC}) was tightened. For the new set of parameter ranges, the sensitivities were dominated by F_{RC}, F_F, and L_{RC}.

- Multiple sensitivity metrics and surrogate model methods were compared for a representative set of responses for Set E. Little difference in rank importance was noted.
- In general, the sensitivity trends for the 6-radial cord configuration followed the 11-cord configuration. Results of different types and locations are important to examine, as evidenced by the out-of-family results for Lobe #5 N_T.
- Future work could focus on demonstration of the capability to support certification with test-validated analyses by: 1) incorporating the NAIPS mid-body fabric and cords; 2) comparing simulation results with existing EDU test data.

Acknowledgements

The authors would like to recognize the contributions of Mr. Alberto Makino (NASA Ames Research Center), who provided the preliminary model and simulation results.

References

1. Lyle, K. H. and Vassilakos, G. J.: Modeling of Global BEAM Structure for Evaluation of MMOD Impacts to Support Development of a Health Monitoring System. NASA/TM-2015-218984. November 2015.
2. Lyle, K. H. and Vassilakos, G. J.: Modeling of Local l BEAM Structure for Evaluation of MMOD Impacts to Support Development of a Health Monitoring System. NASA/TM-2015-218984. November 2015.
3. Lindell, M. C., Hughes, S. J., Dixon, M, and Willey, C. E.: Structural Analysis and Testing of the Inflatable Re-entry Vehicle Experiment (IRVE). Proceedings of the 47th AIAA/ASME/ASCE/AHS/ASC Structures, Structural Dynamics, and Materials Conference, AIAA Paper No. 2006-1699, Newport RI, 1-4 May 2006.
4. Lyle, K. H.: Comparison of Analysis with Test for Static Loading of Two Hypersonic Inflatable Aerodynamic Decelerator Concepts. NASA TM-2015-218778, July 2015.
5. Timmers, R. B.; Hardy, R. C.; and Welch, J. V.: Modeling and Simulation of the Second-Generation Orion Crew Module Air Bag Landing System. Proceeding of the 20th AIAA Aerodynamic Decelerator Systems Technology Conference and Seminar, AIAA Paper No. 2009-2921, Seattle WA, May 4-7, 2009.
6. Tutt, B.; Johnson, R. K.; and Lyle, K.: Development of an Airbag Landing System for the Orion Crew Module. Proceedings of the 10th International LS-Dyna Users Conference, Dearborn MI, June 8-10, 2008.
7. Tutt, B. A.; and Taylor, A. P.: Applications of LS-Dyna to Structural Problems Related to Recovery Systems and Other Fabric Structures. Proceedings of the 7th International LS-Dyna Users Conference, Dearborn MI, May 19-21, 2002.

8. Guide for the Verification and Validation of Computational Fluid Dynamics Simulations. AIAA Publication AIAA G-077-1998, 1998, Reston VA.
9. NASA Standard for Models and Simulations. NASA Publication NASA-STD-7009, 2006.
10. Sandia National Laboratories Predictive Capability Maturity Model for Computational Modeling and Simulation. Sandia Publication SAND-2007-5948, 2007.
11. Iooss B., Lemaître P. (2015) A Review on Global Sensitivity Analysis Methods. In: Dellino G., Meloni C. (eds) Uncertainty Management in Simulation-Optimization of Complex Systems. Operations Research/Computer Science Interfaces Series, vol 59. Springer, Boston, MA
12. Horta, L. G., Reaves, M. C., Jackson, K. E., Annett, M. S. Littell, J. D.: Fuselage Impact Testing and Simulation: A Model Calibration Exercise. Proceedings of the IMAC-XXII A Conference and Exposition on Structural Dynamics, Orlando FL, February 2014.
13. Lyle, K. H.: Preliminary Structural Sensitivity Study of Hypersonic Inflatable Aerodynamic Decelerator Using Probabilistic Methods. NASA TM-2014-218290, July 2014.
14. Jones, T. C.: Structural Certification of Human-Related Inflatable Space Structures. 2018 IEEE Aerospace Conference, 3-10 March 2018, Big Sky MT.
15. Doggett, W. R., Jones, T. C., Watson, J. J., Warren, J. E., Makino, A., Selig, M., and Mikulas, M. M., "Non-Axisymmetric Inflatable Pressure Structure (NAIPS) Concept that Enables Mass Efficient Packageable Pressure Vessels with Openings," 3rd AIAA Spacecraft Structures Conference, 2016 AIAA SciTech Forum and Exposition, AIAA Paper 2016-1475.
16. Jones, T. C., Doggett, W. R., Warren, J. E., Watson, J. J., Shariff, K. I., Makino, A., and Yount, B. C.: Non-Axisymmetric Inflatable Pressure Structure (NAIPS) Full-Scale Pressure Test. 4th AIAA Spacecraft Structures Conference/AIAA SciTech Forum, AIAA Paper 2017-0854, 9-13 January 2017, Grapevine TX.
17. Lyle, K. H. and Jones, T. C.: Demonstration of Probabilistic Sensitivity Analyses Tools on the Structural Response of a Representative Inflatable Space Structure. NASA TM-2018-219826, April 2018.
18. *LS-Dyna Keyword User's Manual*, Version 971, July 27, 2012 (revision: 1617).
19. Halton, J.H.: On the Efficiency of Certain Quasi-Random Sequences of Points in Evaluating Multi-Dimensional Integrals. *Numerische Mathematik*, Vol. 2, 1960, pp. 84–90.
20. Saltelli, A.; Chan, K.; Scott, E. M.: *Sensitivity Analysis*. Chichester, England: John Wiley and Sons, 2000
21. Helton, J. C. and Davis, F. J.: Illustration of Sampling-Based Methods for Uncertainty and Sensitivity Analysis, *Risk Analysis*, Vol 22, No. 3, 2002 pp 591-622.
22. Sobol, I. M., *et al*: Estimating Approximation Error When Fixing Unessential Factors in Global Sensitivity Analysls. *Reliability Engineering and Safety*, Vol. 92, 2007, pp. 957-960.
23. Mullur, A. A. and Messac, A.: Extended Radial Basis Functions: More Flexible and Effective Metamodeling. AIAA Journal, Vol 43, No. 6, June 2005, pp 1306-1315.

24. Montgomery, D. C.: *Design and Analysis of Experiments*. 6th Edition, John Wiley and Sons, 2005.
25. Matlab Release 2015b, The MathWorks, Inc., Natick, Massachusetts, United States.
26. *LS-Opt User's Manual*, Version 5, December 2015.

Table I. Parameter Ranges for Uncertainty Studies.

Set	No. of Radial Cords	F_{RC}		F_F		F_{LC}		L_{RC}, in		Pressure, psi		Friction	
		Lower	Upper	Lower	Upper	Lower	Upper	Lower	Upper	Lower	Upper	Lower	Upper
D	**11**	0.8	2.0	0.8	1.2	0.8	2.0	**104.6**	**108.7**	15	15.4	0	0.02
E	**11**	0.8	2.0	0.8	1.2	0.8	2.0	**107.0**	**107.7**	15	15.4	0	0.02
F	**6**	0.8	2.0	0.8	1.2	0.8	2.0	**104.6**	**108.7**	15	15.4	0	0.02
G	**6**	0.8	2.0	0.8	1.2	0.8	2.0	**107.0**	**107.7**	15	15.4	0	0.02

Table II. Normalized RMS error of Set D ERBF relative to simulations.

Parameter (Cord, Lobe)	P_{RC}, %	F_{LC}, %	N_R, %	N_T, %
1	1.7	1.3	1.2	2.4
2	1.7	1.3	1.2	2.1
3	1.5	1.2	1.2	1.4
4	1.3	N/A	1.1	1.0
5	1.1	N/A	1.3	1.0
6	1.1	N/A	1.2	1.0
7	1.2	N/A	1.4	1.0
8	1.3	N/A	1.7	0.9
9	1.5	N/A	1.9	1.0
10	1.6	N/A	2.1	1.0
11	1.6	N/A	N/A	N/A

Table III. Normalized RMS error of Set F ERBF relative to simulations.

Parameter (Cord, Lobe)	P_{RC}, %	F_{LC}, %	N_R, %	N_T, %
1	0.9	0.8	0.5	5.0
2	0.8	0.8	0.6	1.7
3	0.8	0.8	0.5	1.1
4	0.8	N/A	1.3	5.1
5	0.8	N/A	0.5	29.4
6	0.8	N/A	N/A	N/A

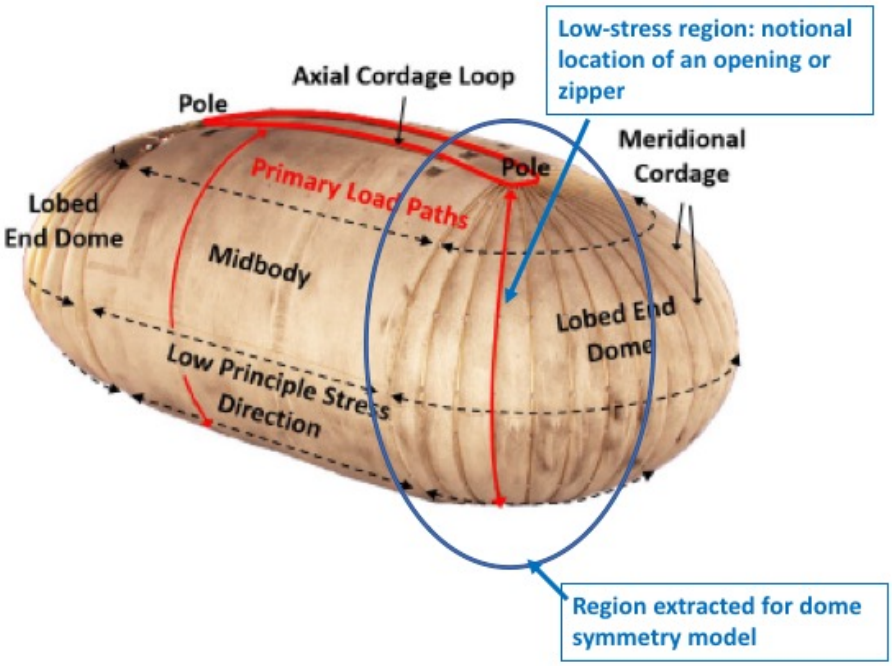

Figure 1. Photograph of inflated NAIPS test article[16].

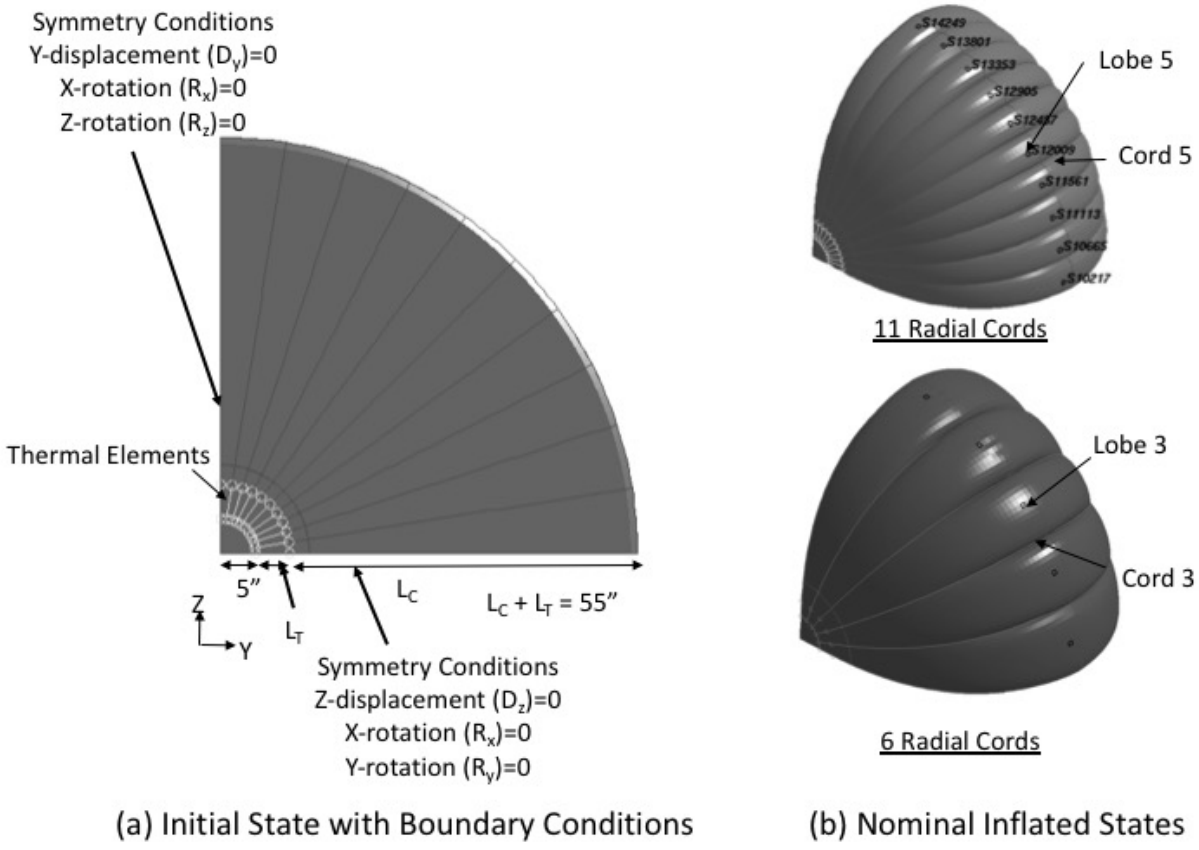

Figure 2. Schematic of dome FEM (D=displacement and R=rotation).

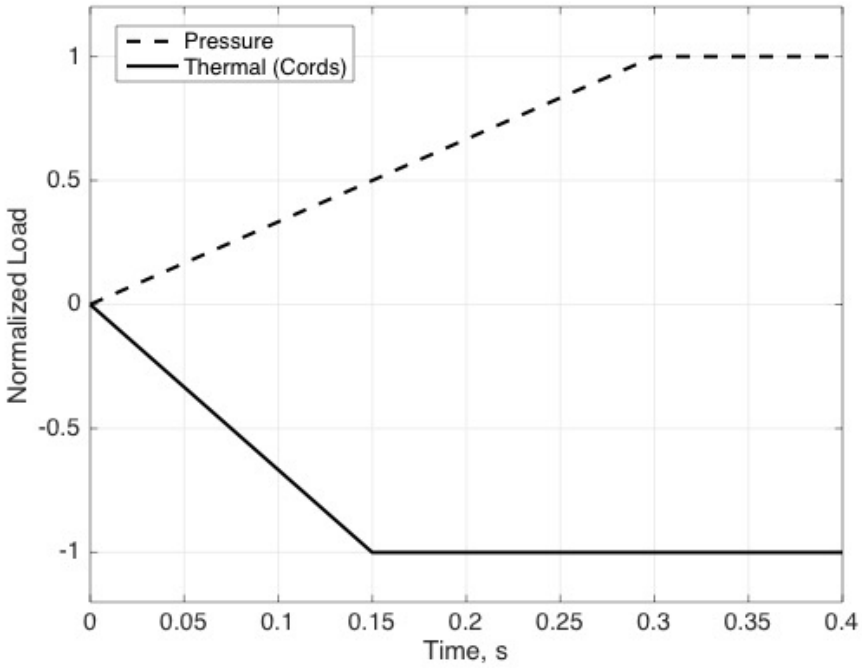

Figure 3. Non-dimensional loading profiles.

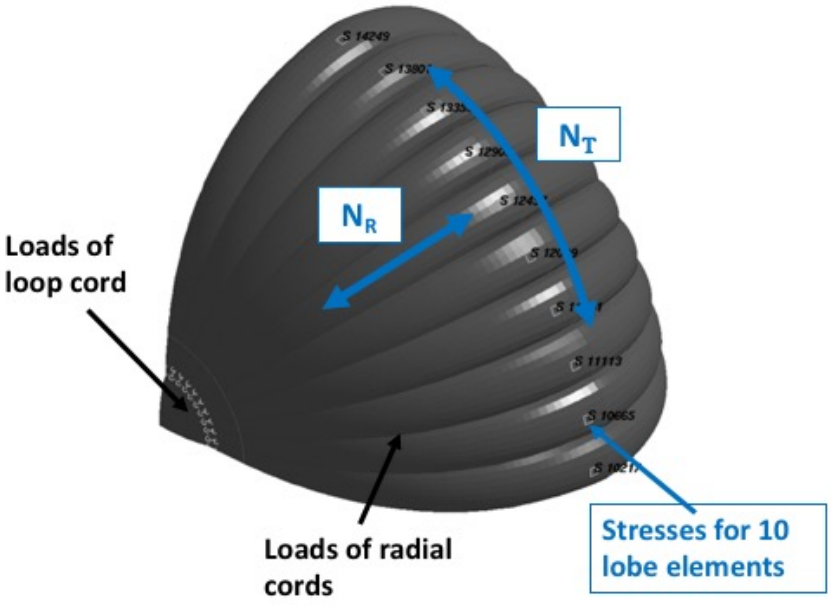

Figure 4. Primary responses of interest.

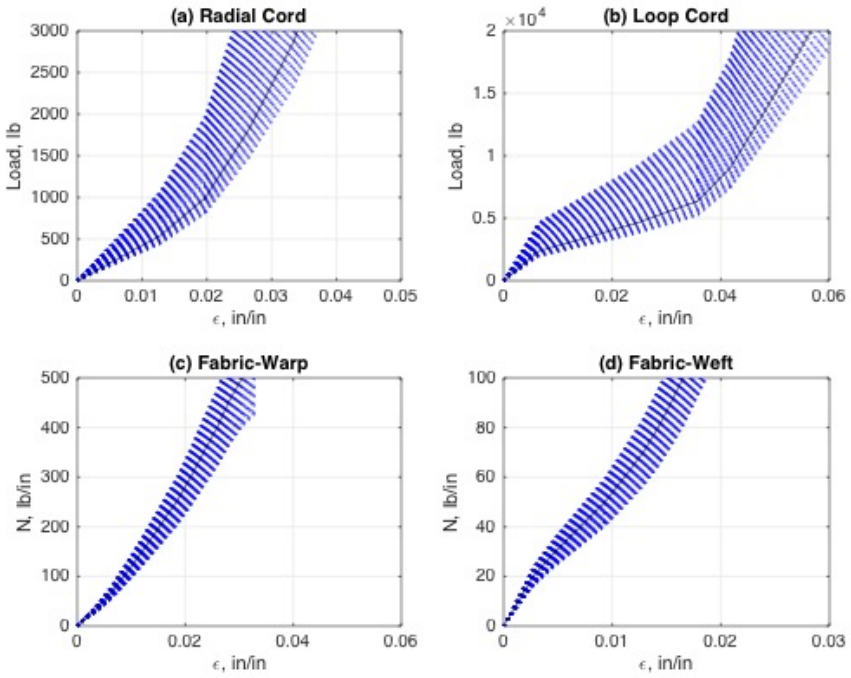

Figure 5. Variation in nonlinear load-strain curves (blue) for input to material property models [Baseline curve is black].

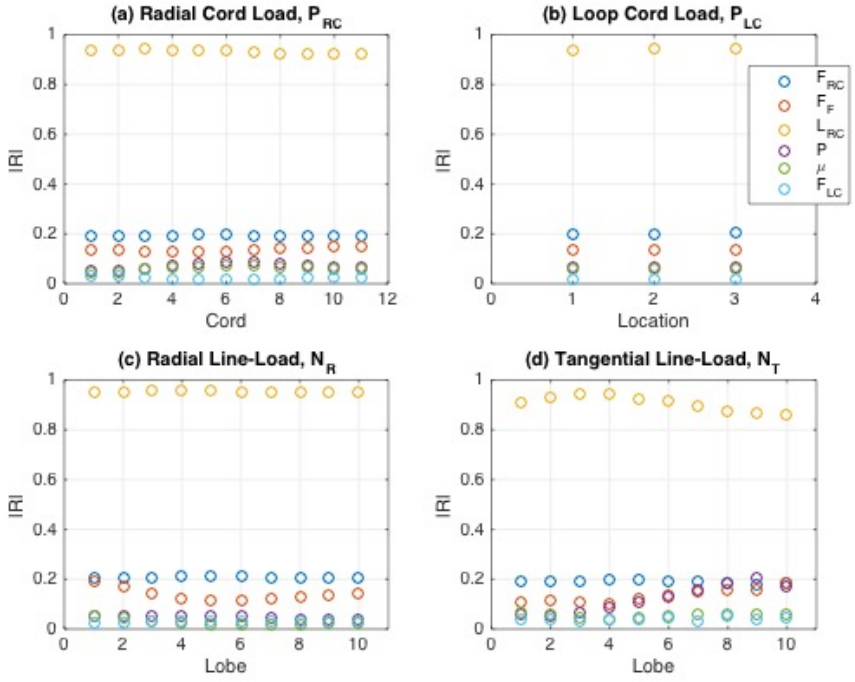

Figure 6. Correlation coefficients for Set D simulations.

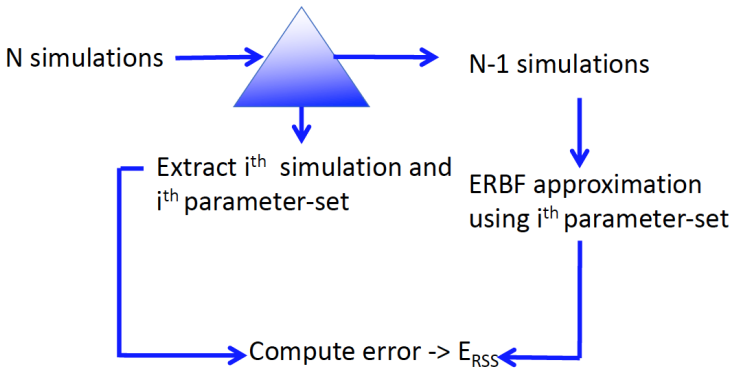

Figure 7. Schematic for ERBF error computation.

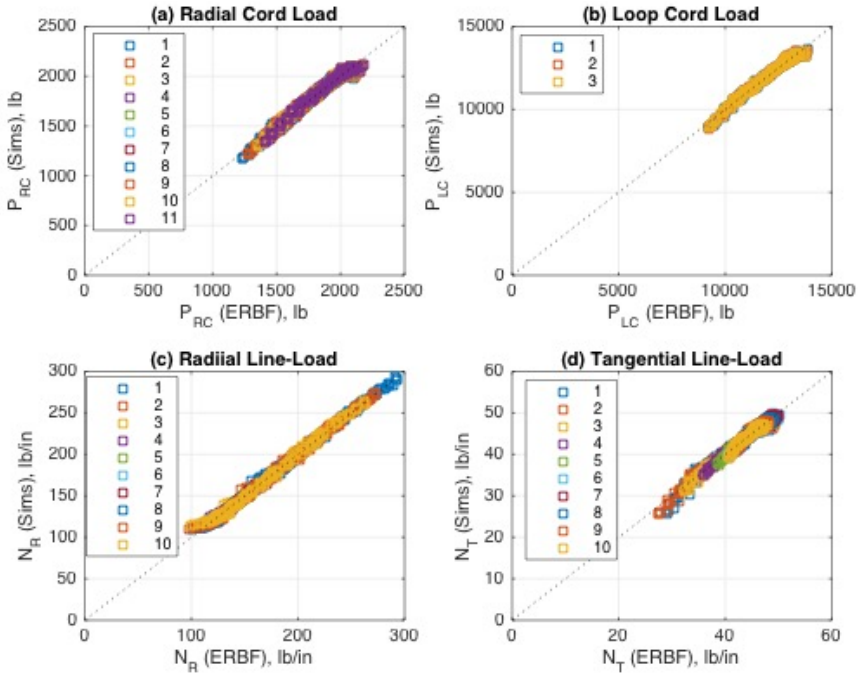

Figure 8. Comparison of simulation and surrogate model results for Set D.

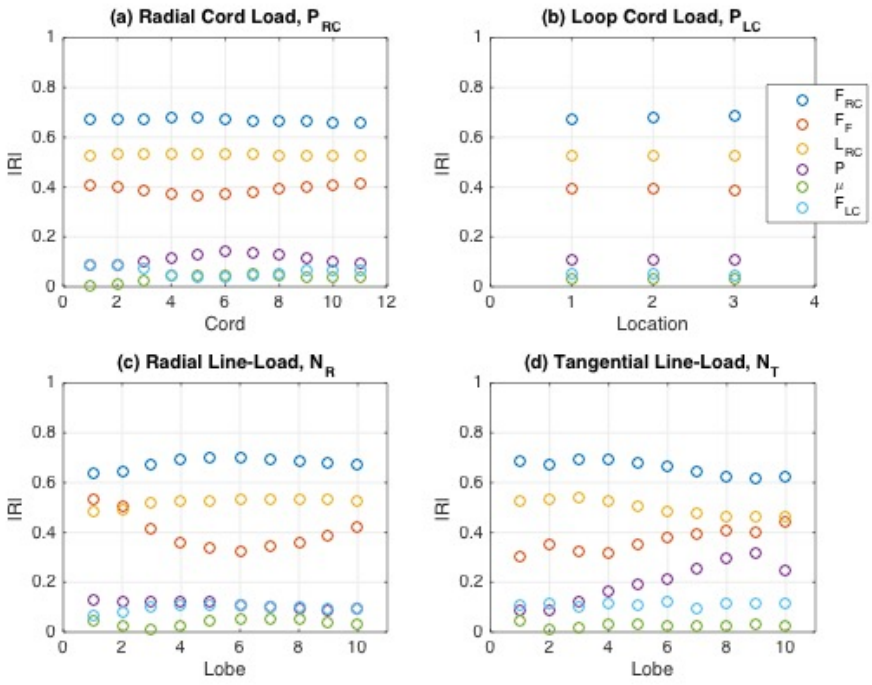

Figure 9. Sensitivity results for Set D ERBF surrogate models evaluated at Set E parameters.

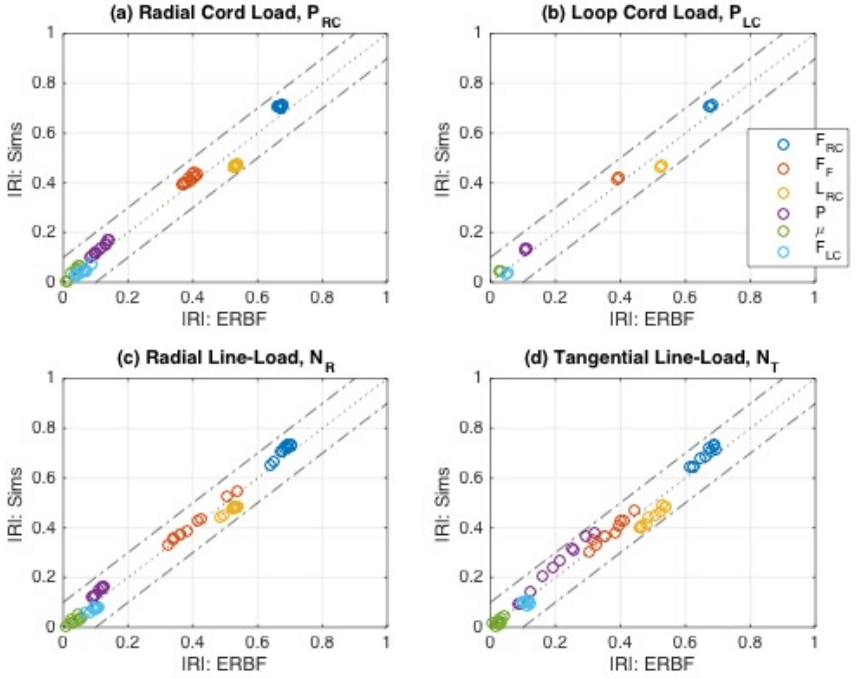

Figure 10. Comparison of sensitivity results: Set E simulations vs Set D ERBF evaluated at Set E parameters.

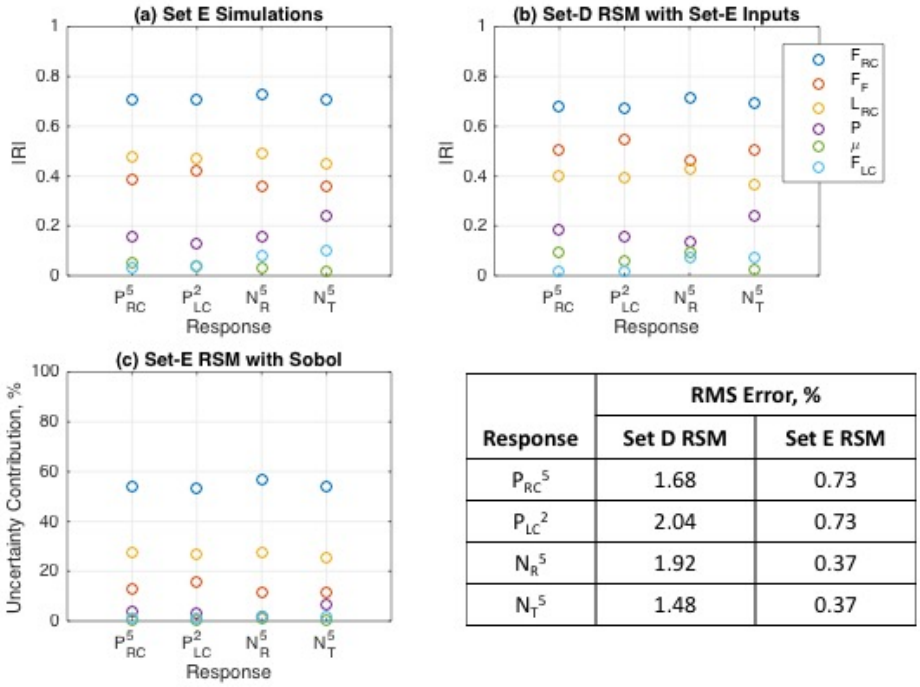

Response	RMS Error, %	
	Set D RSM	Set E RSM
P_{RC}^5	1.68	0.73
P_{LC}^2	2.04	0.73
N_R^5	1.92	0.37
N_T^5	1.48	0.37

Figure 11. Comparison of various sensitivity metrics for Set E parameters.

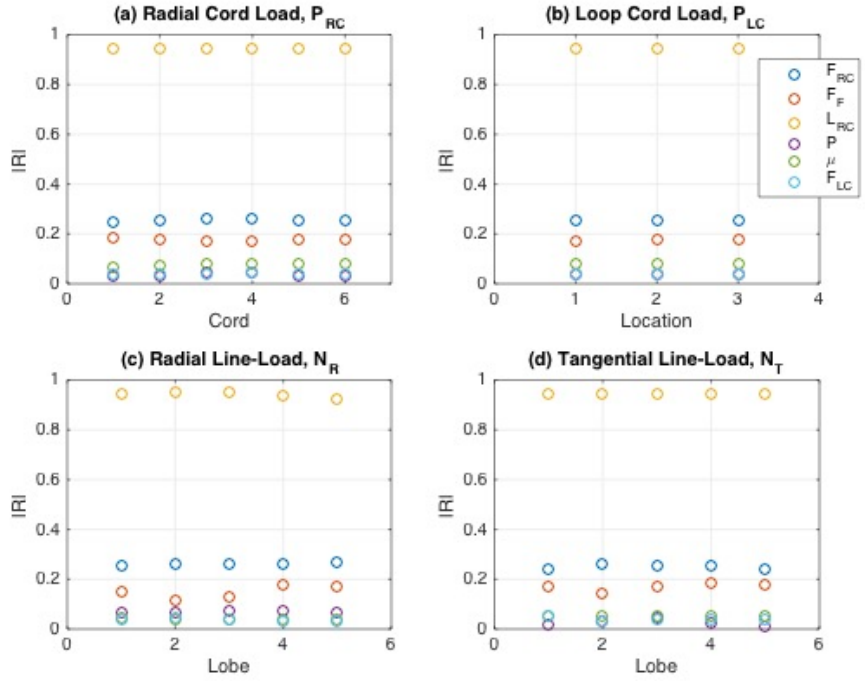

Figure 12. Correlation coefficients for Set F simulations.

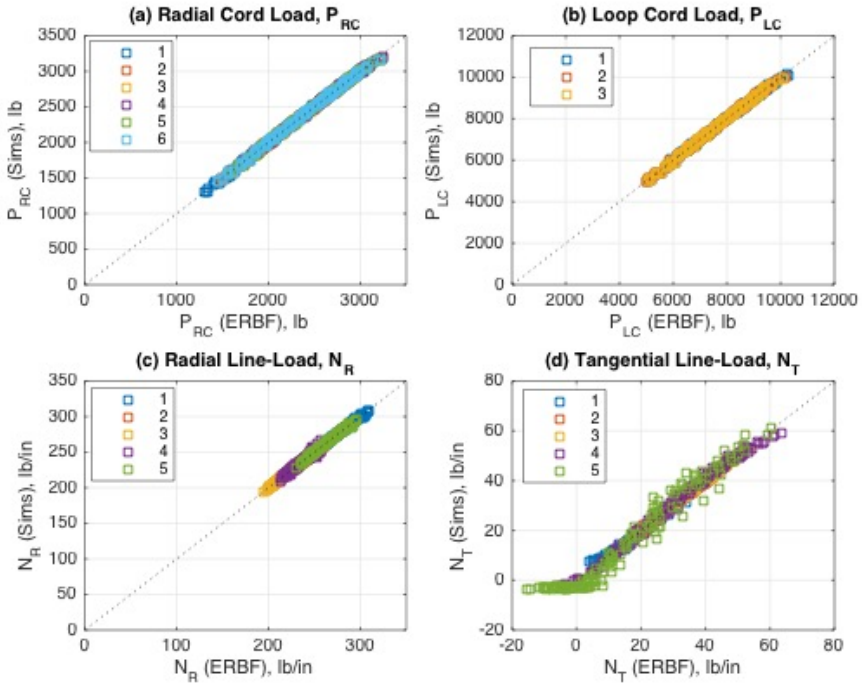

Figure 13. Comparison of simulation and surrogate model results for Set F.

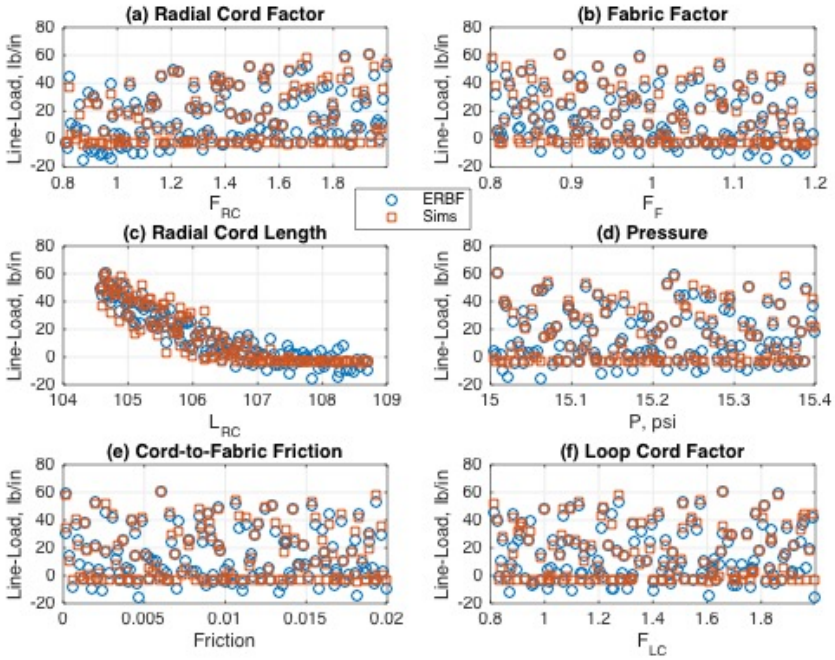

Figure 14. Cross-plot of N_T vs input parameters for Set F/Lobe 5.

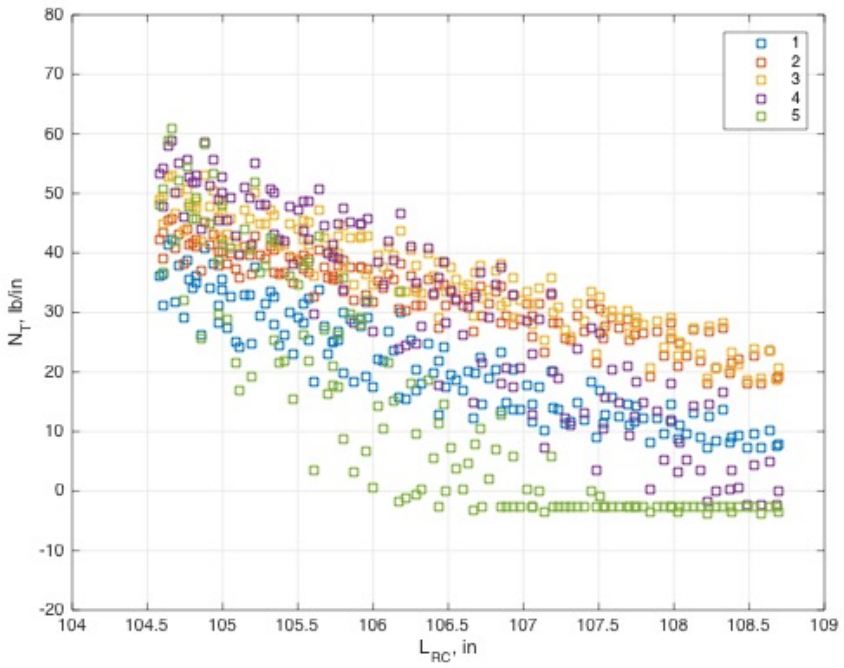

Figure 15. Cross-plot of N_T vs radial cord length (L_{RC}) for each lobe of Set F.

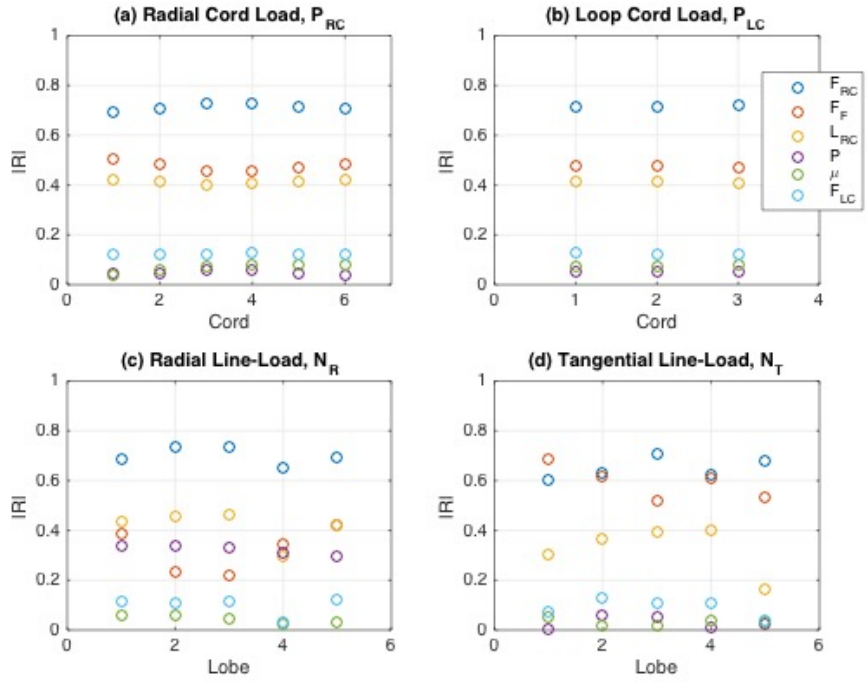

Figure 16. Sensitivity results for Set F ERBF surrogate models evaluated at Set G parameters.

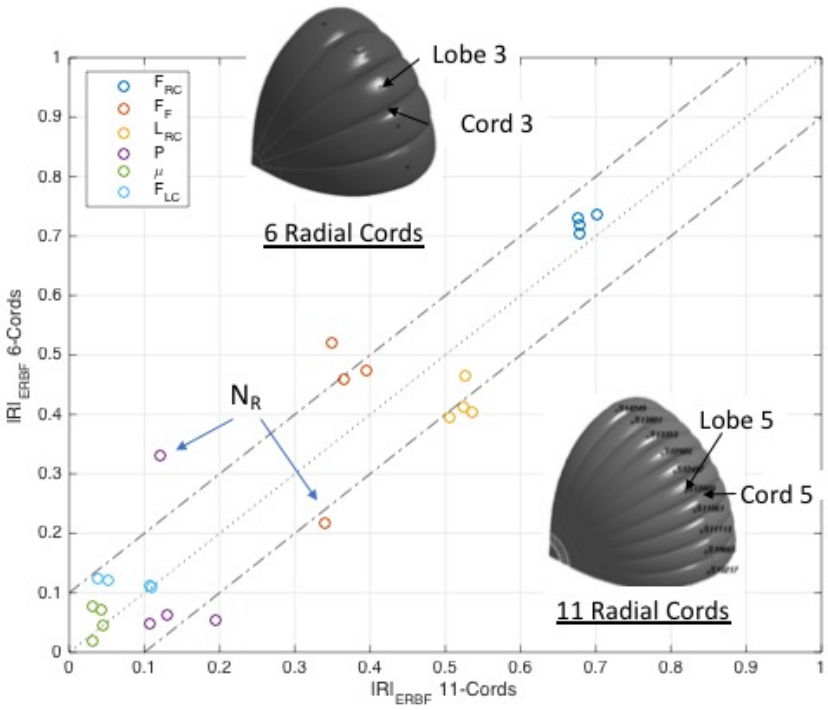

Figure 17. Representative sensitivity results for 11 radial cords (Figure 9) vs 6 radial cords (Figure 16).

REPORT DOCUMENTATION PAGE

Form Approved
OMB No. 0704-0188

1. REPORT DATE *(DD-MM-YYYY)*	2. REPORT TYPE	3. DATES COVERED *(From - To)*
1-08-2018	Technical Memorandum	

4. TITLE AND SUBTITLE

Probabilistic Sensitivity Analyses Incorporating Surrogate Models for the Structural Response of a Representative Inflatable Space Structure

5a. CONTRACT NUMBER

5b. GRANT NUMBER

5c. PROGRAM ELEMENT NUMBER

6. AUTHOR(S)

Lyle, Karen H.; Jones, Thomas C.

5d. PROJECT NUMBER

5e. TASK NUMBER

5f. WORK UNIT NUMBER

089407.01.23

7. PERFORMING ORGANIZATION NAME(S) AND ADDRESS(ES)

NASA Langley Research Center
Hampton, VA 23681-2199

8. PERFORMING ORGANIZATION REPORT NUMBER

L-20952

9. SPONSORING/MONITORING AGENCY NAME(S) AND ADDRESS(ES)

National Aeronautics and Space Administration
Washington, DC 20546-0001

10. SPONSOR/MONITOR'S ACRONYM(S)

NASA

11. SPONSOR/MONITOR'S REPORT NUMBER(S)

NASA-TM-2018-220082

12. DISTRIBUTION/AVAILABILITY STATEMENT

Unclassified
Subject Category 39
Availability: NASA STI Program (757) 864-9658

13. SUPPLEMENTARY NOTES

14. ABSTRACT This study concentrates on results from probabilistic analysis and numerical simulation tools to identify parameter sensitivities and assess surrogate model suitability for a novel inflatable airlock concept, specifically the Non-Axisymmetric Inflatable Pressure Structure (NAIPS) under NASA's Minimalistic Advanced Softgoods Hatch (MASH) Program. The current studies extended the demonstration of probabilistic analysis tools to identify parameter sensitivities by: incorporating nonlinear material load-strain property curves and orthotropic representation of the fabric; and exploring the use of surrogate models to facilitate rapid evaluations as new information becomes available, as well as enable optimizations. The airlock model has been simplified to focus on the end dome section. Brief overviews of the finite element model and associated surrogate models are provided along with the probabilistic sensitivity analysis approaches. Responses of interest include the sensitivities of various loads in the structural elements of the NAIPS to material properties, cord lengths, inflation pressure and friction between softgoods components. The use of surrogate models was explored to facilitate rapid sensitivity evaluations as parameter ranges change. The completion of the sensitivity studies improved understanding of the dependence of load responses to several uncertain parameters and confidence in the ability to use surrogate models to represent the finite element simulations.

15. SUBJECT TERMS

Inflatable space structures; Probabilistic analysis; Softgoods; Structural analysis; Surrogate models

16. SECURITY CLASSIFICATION OF:			17. LIMITATION OF ABSTRACT	18. NUMBER OF PAGES	19a. NAME OF RESPONSIBLE PERSON
a. REPORT	b. ABSTRACT	c. THIS PAGE			STI Help Desk (email: help@sti.nasa.gov)
U	U	U	UU	27	19b. TELEPHONE NUMBER *(Include area code)* (757) 864-9658